Progress In Electromagnetics Research, PIER 91, 53–68, 2009

MODELLING AN IRONLESS LOUDSPEAKER BY USING THREE-DIMENSIONAL ANALYTICAL APPROACHES

R. Ravaud and G. Lemarquand

Laboratoire d'Acoustique de l'Universite du Maine
UMR CNRS 6613, Avenue Olivier Messiaen, Le Mans 72085, France

Abstract—This paper presents some improved three-dimensional expressions of the magnetic field created by tile permanent magnets uniformly and radially magnetized for the design of ironless loudspeaker structures. All the expressions determined have been reduced to compact forms. We use these expressions for the optimization of ironless loudspeaker structures in which the radial field must be radially uniform. Indeed, as ring permanent magnets radially magnetized are rather difficult to manufacture, these magnets are replaced by assemblies of tile permanent magnets radially and uniformly magnetized. We present an example of ironless loudspeaker structure that has been optimized with our three-dimensional approaches.

1. INTRODUCTION

Tile permanent magnets can be used for manufacturing ring permanent magnets radially magnetized by stacking them together. Such a way of manufacturing a ring is commonly realized because ring permanent magnets radially magnetized are difficult to fabricate. Consequently, this alternative method consists in using tile permanent magnets uniformly magnetized. However, they do not exhibit the same properties as tiles radially magnetized and can lower the quality of the radial field created by the permanent magnet structure.

Many authors have studied the field created by ring [1–7], cylinder [8–10], tile permanent magnets [11–13] or by disk conductors [14–16]. All these analytical methods have enabled authors to study the stiffness or the force between permanent magnets for magnetic bearings [17, 18] or couplings [19–22]. More generally, optimizations can be carried out with analytical or semi-analytical

Corresponding author: G. Lemarquand (guy.lemarquand@univ-lemans.fr).

approaches [23–25]. An application of the analytical calculation of the magnetic field produced by permanent magnets is the design of ironless loudspeakers [26–28].

This paper presents improved three-dimensional expressions of the magnetic field created by tile permanent magnets uniformly magnetized. The analytical expressions we present are not only more compact but also simpler to use than the ones determined in [13]. Indeed, the contribution of the magnetic pole surface densities located on the straight faces of the tile permanent magnet can be described in a simpler expression than the one determined in [13]. Even though the two problems are different between this paper and [13], the form of the analytical expressions that must be determined analytically is the same. Then, these expressions are used in order to design an ironless loudspeaker structure.

The first section presents the way of obtaining these analytical expressions by using the Coulombian model. Then, this paper discusses the wave rate of the radial field created by a stacked structure of tile permanent magnets uniformly magnetized. A prototype has been built to show the suitability of such an analytical three-dimensional approach. All the expressions obtained in this paper are available online [29].

2. MODELLING TILE PERMANENT MAGNETS WITH THE COULOMBIAN MODEL

This section presents the geometry studied and the model used for modelling the magnetic field created by tile permanent magnets uniformly magnetized. We explain how to find the surface densities located on the faces of a tile permanent magnet uniformly magnetized. The magnetic polarization of the tile permanent magnet studied is $J = 1\,\mathrm{T}$ for the rest of this paper.

2.1. Modelling the Tile Permanent Magnet Using the Coulombian Approach

The geometry considered and the related parameters are shown in Fig. 1. The Coulombian model asserts that a permanent magnet whose polarization is $\vec{J}$ can be represented by using fictitious magnetic charges which are located inside the magnet and on its faces. Thus, there are both a magnetic pole volume density σ_v^* inside the magnet and a magnetic pole surface density σ_s^* located on its faces. These magnetic pole densities can be determined by using the following expressions:

$$\sigma_v^* = -\vec{\nabla} \cdot \vec{J} \tag{1}$$

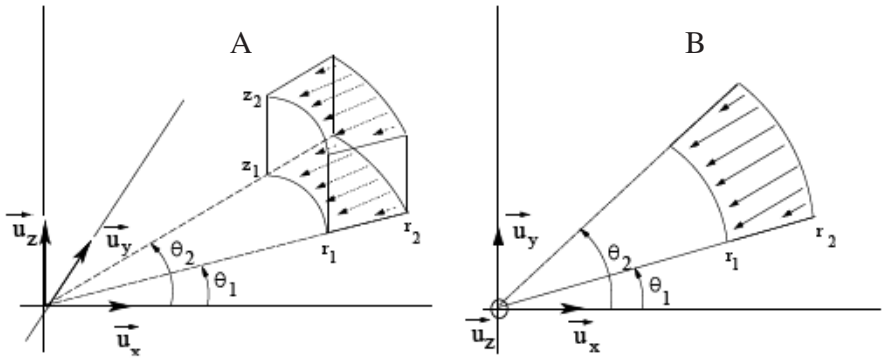

Figure 1. Representation of the configuration considered. The ring inner radius is r_1; the ring outer one is r_2; its height is $z_2 - z_1$; its angular width is $\theta_2 - \theta_1$.

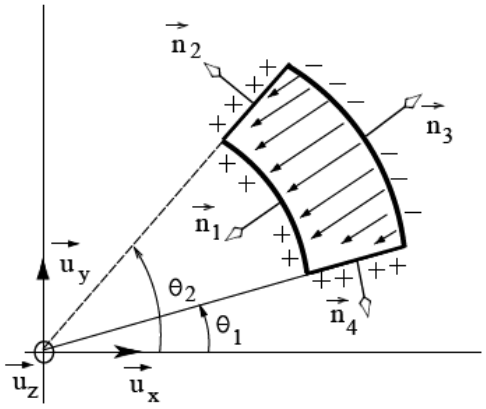

Figure 2. Definition of the unit normal vectors of the tile permanent magnet.

and

$$\sigma_s^* = \vec{J} \cdot \vec{n} \tag{2}$$

Let us now apply (1) and (2) to our geometry shown in Fig. 1. For this purpose, let us consider the geometry shown in Fig. 2 where we have defined the four unit normal vectors in the plane $\vec{u}_x, \vec{u}_y$.

The magnetic polarization vector $\vec{J}$ is expressed as follows:

$$\vec{J} = -J_x \vec{u}_x - J_y \vec{u}_y \tag{3}$$

where $J_x = J\cos\left(\frac{\theta_2+\theta_1}{2}\right)$ and $J_y = J\sin\left(\frac{\theta_2+\theta_1}{2}\right)$. By using (1) with (3), we deduct that:

$$\sigma_v^* = 0 \tag{4}$$

This is a well-known result: a permanent magnet whose magnetic polarisation is uniform does not have any magnetic pole volume densities.

By applying (2) to $\vec{n}_1$, $\vec{n}_2$, $\vec{n}_3$ and $\vec{n}_4$ (see Fig. 2), we find:

$$\begin{aligned}
\vec{J}\cdot\vec{n}_1 &= (-J_x\vec{u}_x - J_y\vec{u}_y)\cdot(-\cos(\theta)\vec{u}_x - \sin(\theta)\vec{u}_y)\\
&= +J\cos\left(\theta - \frac{\theta_1+\theta_2}{2}\right)\\
\vec{J}\cdot\vec{n}_2 &= (-J_x\vec{u}_x - J_y\vec{u}_y)\cdot(-\sin(\theta_2)\vec{u}_x + \cos(\theta_2)\vec{u}_y)\\
&= +J\sin\left(\frac{\theta_2-\theta_1}{2}\right)\\
\vec{J}\cdot\vec{n}_3 &= (-J_x\vec{u}_x - J_y\vec{u}_y)\cdot(+\cos(\theta)\vec{u}_x + \sin(\theta)\vec{u}_y)\\
&= -J\cos\left(\theta - \frac{\theta_1+\theta_2}{2}\right)\\
\vec{J}\cdot\vec{n}_4 &= (-J_x\vec{u}_x - J_y\vec{u}_y)\cdot(+\sin(\theta_1)\vec{u}_x - \cos(\theta_1)\vec{u}_y)\\
&= +J\sin\left(\frac{\theta_2-\theta_1}{2}\right)
\end{aligned} \tag{5}$$

Consequently, the tile permanent magnet is represented by four charged planes.

3. THREE-DIMENSIONAL EXPRESSIONS OF THE MAGNETIC FIELD COMPONENTS CREATED BY A TILE PERMANENT MAGNET UNIFORMLY MAGNETIZED

3.1. Magnetic Field Created by a Tile Permanent Magnet Uniformly Magnetized

The magnetic field created by one tile permanent magnet uniformly magnetized is expressed as follows:

$$\vec{H}(r,\theta,z) = \frac{J}{4\pi\mu_0}\int_{\theta_1}^{\theta_2}\int_{z_1}^{z_2}\cos\left(\tilde{\theta} - \frac{\theta_1+\theta_2}{2}\right)\frac{u(\vec{\tilde{\theta}})}{\left|u(\vec{\tilde{\theta}})\right|^3}r_1 d\tilde{\theta}d\tilde{z}$$

$$-\frac{J}{4\pi\mu_0}\int_{\theta_1}^{\theta_2}\int_{z_1}^{z_2}\cos\left(\tilde{\theta}-\frac{\theta_1+\theta_2}{2}\right)\frac{u(\vec{\tilde{\theta}})}{\left|u(\vec{\tilde{\theta}})\right|^3}r_2 d\tilde{\theta}d\tilde{z}$$
$$+\frac{J}{4\pi\mu_0}\int_{r_1}^{r_2}\int_{z_1}^{z_2}\sin\left(\frac{\theta_2-\theta_1}{2}\right)\frac{u(\vec{\theta}_2)}{\left|u(\vec{\theta}_2)\right|^3}d\tilde{r}d\tilde{z}$$
$$+\frac{J}{4\pi\mu_0}\int_{r_1}^{r_2}\int_{z_1}^{z_2}\sin\left(\frac{\theta_2-\theta_1}{2}\right)\frac{u(\vec{\theta}_1)}{\left|u(\vec{\theta}_1)\right|^3}d\tilde{r}d\tilde{z} \quad (6)$$

where μ_0 is the permeability of the vacuum, J is the magnetic polarization of the tile permanent magnet and $\vec{u}$ is expressed as follows:

$$\vec{u}(\theta_i)=(r-r_j\cos(\theta-\theta_i)\vec{u}_x-r_j\sin(\theta-\theta_i)\vec{u}_y+(z-\tilde{z})\vec{u}_z \quad (7)$$

where $j=r_1$ when $dS=r_1 d\tilde{\theta}d\tilde{z}$ (the inner surface) or $j=r_2$ when $dS=r_2 d\tilde{\theta}d\tilde{z}$ (the outer surface). The integration of (6) leads to the magnetic field components along the three defined axes: $H_r(r,\theta,z)$, $H_\theta(r,\theta,z)$ and $H_z(r,\theta,z)$ (expressed in A/m) which are given by (11), (14) and (17). We use the relations $x_k=\cos(\theta-\theta_k)$, $x_{2k}=\cos(2(\theta-\theta_k))$, $y_k=\sin(\theta_k-\theta)$ and $t_k=\cot(\theta-\theta_k)$. In addition, we define $\xi_{i,j}$, $\eta_{i,k}$ and $\alpha_{i,j,k}$ as follows:

$$\xi_{i,j}=\sqrt{r^2+r_i^2+(z-z_j)^2-2rr_i\cos(\theta-\tilde{\theta})} \quad (8)$$
$$\eta_{i,k}=\sqrt{2r_i^2-4rr_ix_k+r^2(1+x_{2k})} \quad (9)$$
$$\alpha_{i,j,k}=\sqrt{r^2+r_i^2-2rr_ix_k+(z-z_j)^2} \quad (10)$$

3.2. Radial Component $H_r(r,\theta,z)$

The radial component $H_r(r,\theta,z)$ of the magnetic field created by one tile permanent magnet uniformly magnetized can be expressed as follows:

$$H_r(r,\theta,z)=\frac{J}{4\pi\mu_0}\sum_{i=1}^{2}\sum_{j=1}^{2}(-1)^{(i+j)}\wp^{(1,r)}(i,j)$$
$$+\frac{J}{4\pi\mu_0}\sum_{i=1}^{2}\sum_{j=1}^{2}\sum_{k=1}^{2}(-1)^{(i+j)}\wp^{(2,r)}(i,j,k) \quad (11)$$

with

$$\wp^{(1,r)}(i,\ j)=\int_{\theta_1}^{\theta_2}\frac{r_i(z_j-z)\left(-r+r_i\cos\left(\theta-\tilde{\theta}\right)\right)\cos\left(\frac{\theta_1+\theta_2-2\tilde{\theta}}{2}\right)}{\left(r^2+r_i^2-2rr_i\cos\left(\theta-\tilde{\theta}\right)\right)\xi_{i,j}}d\tilde{\theta} \tag{12}$$

$$\wp^{(2,r)}(i,j,k)=-\frac{r\left(rx_k(x_{2k}-1)+2r_iy_k^2\right)}{\sqrt{-r^2(-1+x_{2k})}\eta_{i,k}}\arctan\left[\frac{(z-z_j)\eta_{i,k}}{\sqrt{-r^2(x_{2k}-1)}\alpha_{i,j,k}}\right] -x_k\log[z-z_j+\alpha_{i,\,j,\,k}] \tag{13}$$

3.3. Azimuthal Component $H_\theta(r,\theta,z)$

The azimuthal component $H_\theta(r,\theta,z)$ of the magnetic field created by one tile permanent magnet uniformly magnetized can be expressed as follows:

$$\begin{aligned}H_\theta(r,\ \theta,\ z)\ =\ &\frac{J}{4\pi\mu_0}\sum_{i=1}^{2}\sum_{j=1}^{2}(-1)^{(i+j)}\wp^{(1,\,\theta)}(i,\ j)\\ &+\frac{J}{4\pi\mu_0}\sum_{i=1}^{2}\sum_{j=1}^{2}\sum_{k=1}^{2}(-1)^{(i+j)}\wp^{(2,\,\theta)}(i,\ j,\ k)\end{aligned} \tag{14}$$

with

$$\wp^{(1,\,\theta)}(i,\ j)=\int_{\theta_1}^{\theta_2}\frac{r_i^2(z-z_j)\sin\left(\theta-\tilde{\theta}\right)\cos\left(\frac{\theta_1+\theta_2-2\tilde{\theta}}{2}\right)}{\xi_{i,j}\left(r^2+r_i^2-2rr_i\cos\left(\theta-\tilde{\theta}\right)\right)}d\tilde{\theta} \tag{15}$$

and

$$\begin{aligned}\wp^{(2,\,\theta)}(i,\ j,\ k)\ =\ &\frac{z-z_j}{\alpha_{i,\,j,\,k}}y_k\sin\left(\frac{\theta_2-\theta_1}{2}\right)\\ &-\frac{r_iy_kt_k}{\alpha_{i,\,j,\,k}}\sin\left(\frac{\theta_2-\theta_1}{2}\right)\arctan\left[\frac{z-z_j}{ry_k}\right]\\ &+\frac{ry_kx_kt_k}{\alpha_{i,\,j,\,k}}\sin\left(\frac{\theta_2-\theta_1}{2}\right)\arctan\left[\frac{z-z_j}{ry_k}\right]\end{aligned} \tag{16}$$

3.4. Axial Component $H_z(r,\theta,z)$

The axial component $H_z(r,\theta,z)$ of the magnetic field created by one tile permanent magnet uniformly magnetized can be expressed as follows:

$$H_z(r,\theta,z) = \frac{J}{4\pi\mu_0}\sum_{i=1}^{2}\sum_{j=1}^{2}(-1)^{(i+j)}\wp^{(1,z)}(i,j) + \frac{J}{4\pi\mu_0}\sum_{i=1}^{2}\sum_{j=1}^{2}\sum_{k=1}^{2}(-1)^{(i+j)}\wp^{(2,z)}(i,\,j,\,k) \quad (17)$$

with

$$\wp^{(1,\,z)}(i,\,j) = \int_{\theta_1}^{\theta_2}\frac{-r_i}{\xi_{i,j}}\cos\left(\frac{\theta_1+\theta_2-2\tilde{\theta}}{2}\right)d\tilde{\theta} \quad (18)$$

and

$$\wp^{(2,\,z)}(i,\,j,\,k) = \sin\left(\frac{\theta_2-\theta_1}{2}\right)\log\left[r_i - r\cos(\theta-\theta_k)+\xi_{i,\,j}\right] \quad (19)$$

3.5. Comparison of the Magnetic Field Created by a Tile Permanent Radially Magnetized and a Tile Permanent Magnet Whose Polarization is Both Uniform and Radial

Tile permanent magnets whose polarization is both uniform and radial are generally used instead of tile permanent magnets radially magnetized (Fig. 3). However, the magnetic field they produce exhibits some differences and thus can lower the quality of the permanent magnet devices.

The three components of the magnetic field created by each tile permanent magnet (radially or uniformly magnetized) are represented in Fig. 4.

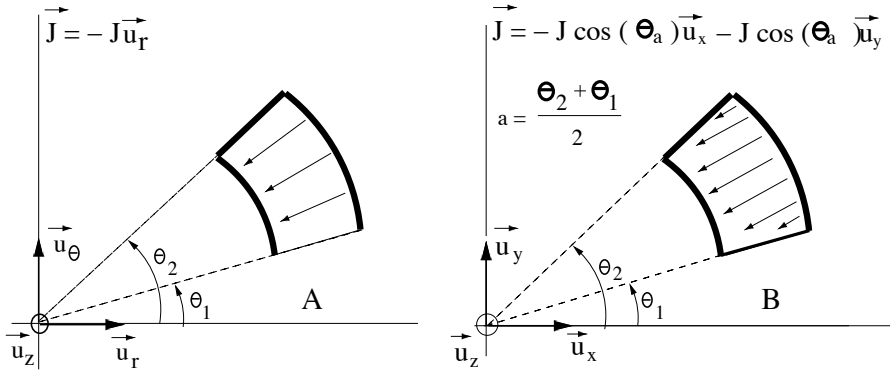

Figure 3. Representation of two tile permanent magnets: the left one is radially magnetized, the right one is uniformly magnetized.

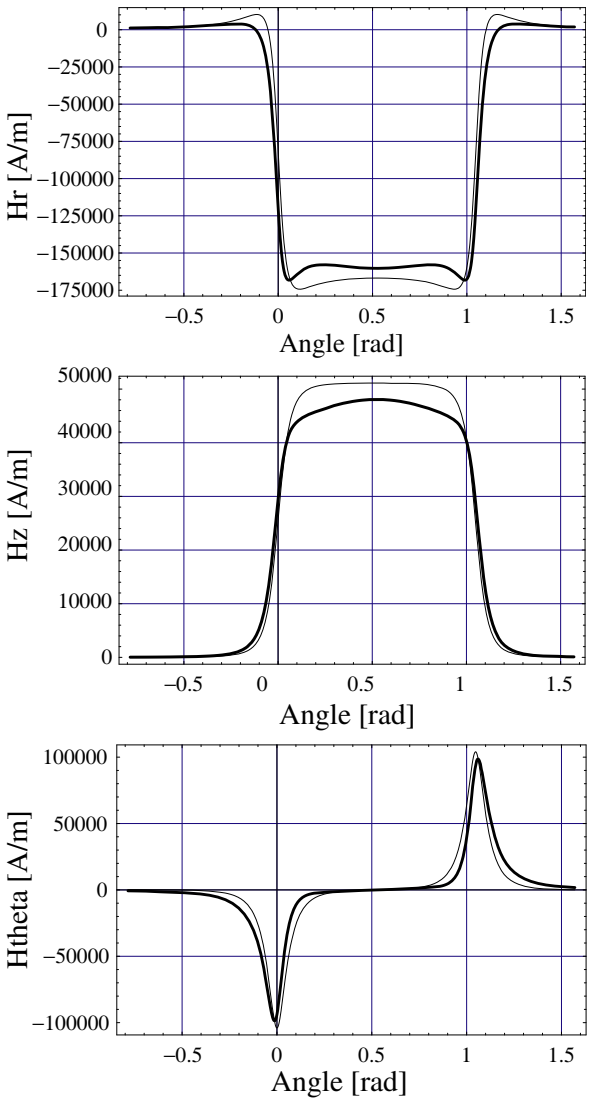

Figure 4. Representation of the the radial, axial and azimuthal components of the magnetic field created by a tile which is either radially magnetized (thin line) or uniformly magnetized (thick line). $r_{in} = 0.025\,\mathrm{m}$, $r_{out} = 0.028\,\mathrm{m}$, $z_b - z_a = 0.003\,\mathrm{m}$, $z = 0.0015\,\mathrm{m}$, $r = 0.024\,\mathrm{m}$ and $\theta_2 - \theta_1 = \frac{\pi}{3}\,\mathrm{rad}$.

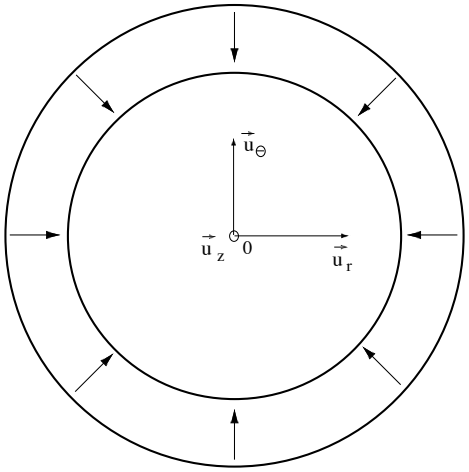

Figure 5. Ring permanent magnet radially magnetized.

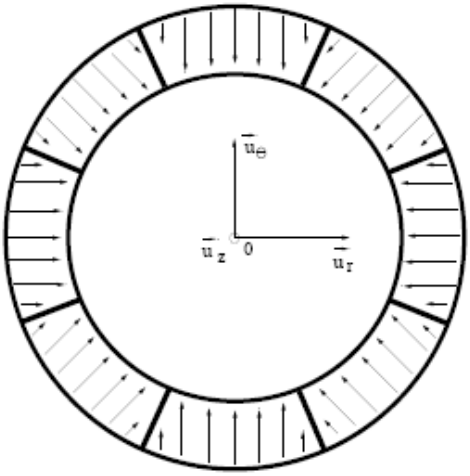

Figure 6. Assembly of several tile permanent magnets uniformly magnetized; the vector magnetization is collinear with the line cutting the middle of each tile permanent magnet.

4. ASSEMBLY OF TILE PERMANENT MAGNETS UNIFORMLY MAGNETIZED FOR CREATING A RING PERMANENT MAGNET

4.1. Study of the Wave Rate Versus the Number of Tile Permanent Magnets Used

The stacking of several tile permanent magnets uniformly magnetized can be used for creating the same radial field as the one created by

a ring permanent magnet radially magnetized. Strictly speaking, the radial field undulates in front of the tile magnets, especially at the place where two tiles are stacked. We propose here to determine the wave rate of the radial field created by the ring of stacked tile permanent magnets versus the number of tiles used. The wave rate WR is defined by

$$WR = \frac{1}{2H_{r_{moy}}} \left(|Sup[H_r]| - |Inf[H_r]| \right) \tag{20}$$

where $H_{r_{moy}}$ is the mean radial field at a given radial distance and a given axial distance from the ring stacked with tile permanent magnets uniformly magnetized.

We study three configurations owing 8, 16 and 32 tile permanent magnets uniformly magnetized. Each tile has the same dimensions. We take the following dimensions for all the illustrative examples: the inner radius r_1 is 0.025 m; the outer radius r_2 is 0.028 m; the height $z_2 - z_1$ is 0.003 m and $J = 1$ T; the observation radial distance is $r = 0.024$ m and the observation axial distance is $z = 0.001$ m. We represent in Fig. 7 the radial field for the three configurations.

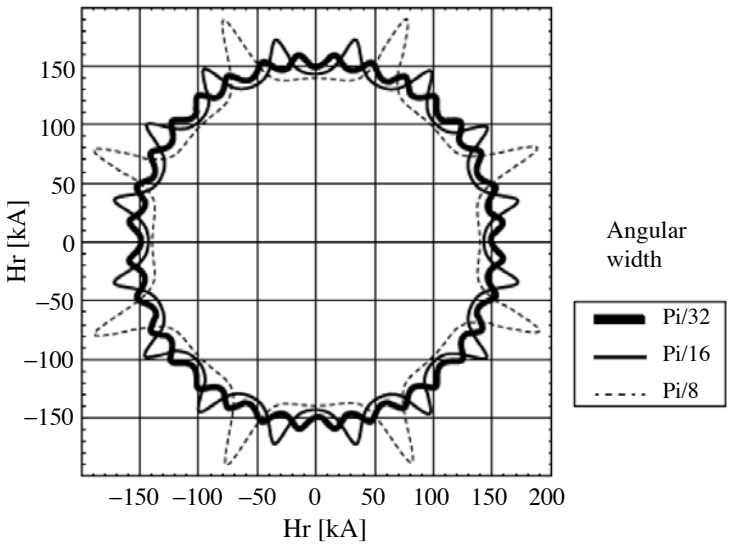

Figure 7. Representation of the radial field created by a ring of stacked tile permanent magnets uniformly magnetized. The inner radius is 0.025 m; the outer radius is 0.028 m; the height is 0.003 m and $J = 1$ T. (Thick line: $\theta_2 - \theta_1 = \frac{\pi}{32}$ rad, thin line: $\theta_2 - \theta_1 = \frac{\pi}{16}$ rad, dashed line: $\theta_2 - \theta_1 = \frac{\pi}{8}$ rad).

Figure 7 clearly shows that the higher is the number of tile permanent magnets used, the lower is the wave rate of the radial field. We can extend this remark when we use N tile permanent magnets uniformly magnetized. Fig. 8 represents the wave rate of the radial field created by a ring of stacked tile permanent magnets versus the number of tiles used. Such a representation is useful because it gives interesting information about how many tile permanent magnets should be used if the wave rate must be inferior to a given percentage.

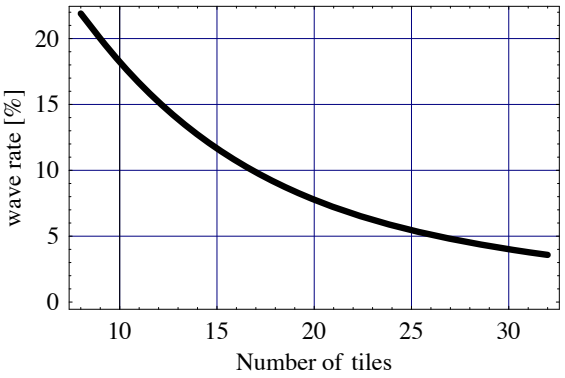

Figure 8. Representation of the wave rate of the radial field created by a ring of stacked tile permanent magnets uniformly magnetized versus the number of tiles used. For each tile, the inner radius is 0.025 m; the outer radius is 0.028 m; the height is 0.003 m.

In addition, when $N \to \infty$, we find the same radial field value as the one determined by Babic and Akyel [4].

5. ILLUSTRATION: DESIGN OF AN IRONLESS LOUDSPEAKER STRUCTURE

This section presents an example of utilization of the expressions determined in this paper. To do so, let us consider a typical ironless structure made of tile permanent magnets stacked together for creating a radial field in the air gap as shown in Fig. 9. In this optimized configuration, this ironless loudspeaker is composed of three ring permanent magnets made of 16 tile permanent magnets uniformly and radially magnetized.

As stated previously, the radial field undulates versus θ. By using the analytical expressions determined in this paper, we can optimize the tile permanent magnet dimensions for obtaining the magnetic field whose undulation is less important. However, the number of

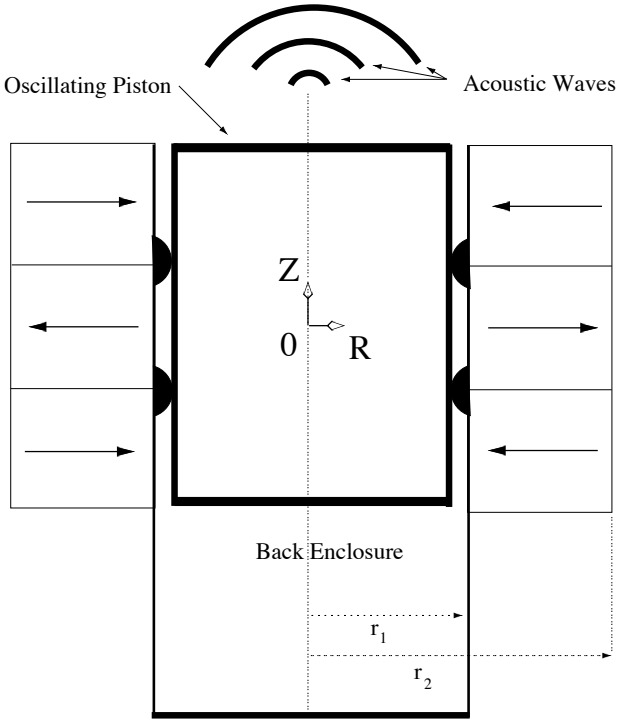

Figure 9. Representation of an ironless loudspeaker with three ring permanent magnets and two ferrofluid seals

tile permanent magnets used must be as small as possible. As it is both difficult and expensive to stack a large number of tile permanent magnets together, we must look for an optimal configuration that creates a radial field whose wave undulation is as small as possible though the number of tile permanent magnets used is as small as possible too. The height of the tile permanent magnets is fixed in our configuration ($h = 3\,\text{mm}$) and the radial width of each tile permanent magnet equals $r_2 - r_1 = 3\,\text{mm}$. Therefore, the only parameter that can be otpimized is the angular width of each tile permanent magnet, that is, the number of tile permanent magnets used in the ironless loudspeaker structure.

This optimization has been performed by using the three-dimensional analytical expressions determined in this paper and the expression of the wave undulation defined in (20). The wave undulation must be inferior to at least 10%. The radial field created $\vec{H}$ is used for two different purposes. First, it is used for moving the emissive piston

shown in Fig. 9 by using the Laplace's force defined as follows:

$$\vec{F}_L = I(t)d\vec{l} \wedge (\mu_0 \vec{H}) \tag{21}$$

where $I(t)$ is the current in the coil that is located on the emissive piston and l is the length of the coil wire. The second objective of this radial field is to contribute to the creation of a ferrofluid seal. Indeed, the magnetic field created by such a structure can be used for creating two ferrofluid seals whose shapes directly influence the mechanical properties of the emissive oscillating piston. The shape of this ferrofluid seal depends on the magnetic pressure that is defined as follows:

$$p_m(r,z) = \mu_0 M \sqrt{H_r(r,\theta,z)^2 + H_\theta(r,\theta,z)^2 + H_z(r,\theta,z)^2} \tag{22}$$

Therefore, the final shape of the ferrofluid seal does not undulate as the radial field as shown in Fig. 7. However, the radial field is the most important component that contributes to the deformation of the seal shape. We present in Fig. 10 an example of prototypes that has been built and optimized in our laboratory.

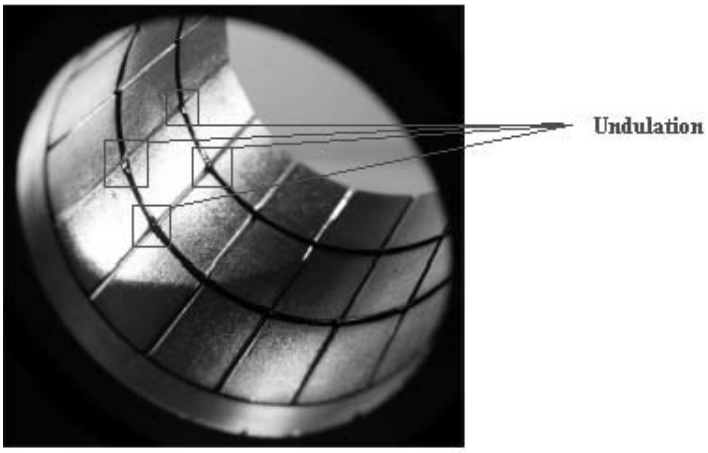

Figure 10. Photography of the ironless loudspeaker structure: we have used 3 times 16 tile permanent magnets for creating two ferrofluid seals; therefore we have $\theta_2 - \theta_1 = \frac{\pi}{8}$ rad; $r_1 = 0.02485$ m, $r_2 = 0.04485$ m, $z_2 - z_1 = 0.02$ m.

As shown in Fig. 10, between two tile permanent magnets, we see the undulation of the magnetic field that stems mainly from the radial field undulation. This behaviour is predicted theoretically with the analytical expressions determined in Section 2.

6. CONCLUSION

This paper has presented improved three-dimensional analytical expressions of the components of the magnetic field created by tile permanent magnets uniformly and radially magnetized. First, we have presented the expressions of the three components $H_r(r, \theta, z)$, $H_\theta(r, \theta, s)$ and $H_z(r, \theta, z)$ created by a tile uniformly magnetized in a compact form. Such expressions are important for practical purposes because tile permanent magnets uniformly magnetized can be used to manufacture a entire ring radially magnetized. Indeed, they are easier to fabricate than arc-shaped permanent magnets radially magnetized. In addition, we have seen that the wave rate of the radial field created by a stacked magnet structure depends directly on the number of tile permanent magnets used. The more we use tile permanent magnets uniformly magnetized, the less the wave rate is important. This element of information can be very useful for manufacturers involved in the design of ironless loudspeakers. We have built an ironless loudspeaker prototype with an optimized number of tile permanent magnets. The effects observed experimentally are well predicted theoretically. As the expressions determined in this paper have a very low computational cost, they can be easily used for optimizing ironless structures.

REFERENCES

1. Durand, E., *Magnetostatique*, Masson Editeur, Paris, France, 1968.
2. Furlani, E. P., *Permanent Magnet and Electromechanical Devices: Materials, Analysis and Applications*, Academic Press, 2001.
3. Babic, S., C. Akyel, and M. M. Gavrilovic, "Calculation improvement of 3D linear magnetostatic field based on fictitious magnetic surface charge," *IEEE Trans. Magn.*, Vol. 36, No. 5, 3125–3127, 2000.
4. Babic, S. and C. Akyel, "Improvement in the analytical calculation of the magnetic field produced by permanent magnet rings," *Progress In Electromagnetics Research C*, Vol. 5, 71–82, 2008.
5. Lemarquand, G. and V. Lemarquand, "Annular magnet position sensor," *IEEE. Trans. Magn.*, Vol. 26, No. 5, 2041–2043, 1990.
6. Ravaud, R., G. Lemarquand, V. Lemarquand, and C. Depollier, "Discussion about the analytical calculation of the magnetic field created by permanent magnets," *Progress In Electromagnetics Research B*, Vol. 11, 281–297, 2009.

7. Ravaud, R., G. Lemarquand, V. Lemarquand, and C. Depollier, "Analytical calculation of the magnetic field created by permanent-magnet rings," *IEEE Trans. Magn.*, Vol. 44, No. 8, 1982–1989, 2008.
8. Furlani, E. P., S. Reznik, and A. Kroll, "A three-dimensonal field solution for radially polarized cylinders," *IEEE Trans. Magn.*, Vol. 31, No. 1, 844–851, 1995.
9. Selvaggi, J. P., S. Salon, O. M. Kwon, M. V. K. Chari, and M. DeBortoli, "Computation of the external magnetic field, near-field or far-field from a circular cylindrical magnetic source using toroidal functions," *IEEE Trans. Magn.*, Vol. 43, No. 4, 1153–1156, 2007.
10. Selvaggi, J. P., S. Salon, O. M. Kwon, and M. V. K. Chari, "Computation of the three-dimensional magnetic field from solid permanent-magnet bipolar cylinders by employing toroidal harmonics," *IEEE Trans. Magn.*, Vol. 43, No. 10, 3833–3839, 2007.
11. Furlani, E. P., "Field analysis and optimization of ndfeb axial field permanent magnet motors," *IEEE Trans. Magn.*, Vol. 33, No. 5, 3883–3885, 1997.
12. Ravaud, R., G. Lemarquand, V. Lemarquand, and C. Depollier, "The three exact components of the magnetic field created by a radially magnetized tile permanent magnet," *Progress In Electromagnetics Research*, PIER 88, 307–319, 2008.
13. Ravaud, R., G. Lemarquand, V. Lemarquand, and C. Depollier, "Magnetic field produced by a tile permanent magnet whose polarization is both uniform and tangential," *Progress In Electromagnetics Research B*, Vol. 13, 1–20, 2009.
14. Azzerboni, B. and E. Cardelli, "Magnetic field evaluation for disk conductors," *IEEE Trans. Magn.*, Vol. 29, No. 6, 2419–2421, 1993.
15. Azzerboni, B. and G. Saraceno, "Three-dimensional calculation of the magnetic field created by current-carrying massive disks," *IEEE Trans. Magn.*, Vol. 34, No. 5, 2601–2604, 1998.
16. Conway, J., "Noncoaxial inductance calculations without the vector potential for axisymmetric coils and planar coils," *IEEE Trans. Magn.*, Vol. 44, No. 10, 453–462, 2008.
17. Delamare, J., E. Rulliere, and J. P. Yonnet, "Classification and synthesis of permanent magnet bearing configurations," *IEEE Trans. Magn.*, Vol. 31, No. 6, 4190–4192, 1995.
18. Moser, R., J. Sandtner, and H. Bleuler, "Optimization of repulsive passive magnetic bearings," *IEEE. Trans. Magn.*, Vol. 42, No. 8, 2038–2042, 2006.

19. Yonnet, J. P., S. Hemmerlin, E. Rulliere, and G. Lemarquand, "Analytical calculation of permanent magnet couplings," *IEEE Trans. Magn.*, Vol. 29, No. 6, 2932–2934, 1993.
20. Charpentier, J. F. and G. Lemarquand, "Calculation of ironless permanent magnet coupling using semi-numerical magnetic pole theory method," *COMPEL*, Vol. 20, No. 1, 72–89, 2001.
21. Lemarquand, V., J. F. Charpentier, and G. Lemarquand, "Nonsinusoidal torque of permanent-magnet couplings," *IEEE Trans. Magn.*, Vol. 35, No. 5, 4200–4205, 1999.
22. Elies, P. and G. Lemarquand, "Analytical study of radial stability of permanent magnet synchronous couplings," *IEEE Trans. Magn.*, Vol. 35, No. 4, 2133–2136, 1999.
23. Perigo, E., R. Faria, and C. Motta, "General expressions for the magnetic flux density produced by axially magnetized toroidal permanent magnets," *IEEE Trans. Magn.*, Vol. 43, No. 10, 3826–3832, 2008.
24. Rakotoarison, H. L., J. P. Yonnet, and B. Delinchant, "Using coulombian approach for modeling scalar potential and magnetic field of a permanent magnet with radial polarization," *IEEE Trans. Magn.*, Vol. 43, No. 4, 1261–1264, 2007.
25. Zhilichev, Y., "Calculation of magnetic field of tubular permanent magnet assemblies in cylindrical bipolar coordinates," *IEEE Trans. Magn.*, Vol. 43, No. 7, 3189–3195, 2007.
26. Berkouk, M., V. Lemarquand, and G. Lemarquand, "Analytical calculation of ironless loudspeaker motors," *IEEE Trans. Magn.*, Vol. 37, No. 2, 1011–1014, 2001.
27. Lemarquand, G., "Ironless loudspeakers," *IEEE Trans. Magn.*, Vol. 43, No. 8, 3371–3374, 2007.
28. Ravaud, R., G. Lemarquand, V. Lemarquand, and C. Depollier, "Ironless loudspeakers with ferrofluid seals," *Archives of Acoustics*, Vol. 33, No. 4, 3–10, 2008.
29. http://www.univ-lemans.fr/∼glemar.